

Microseismic monitoring using SADAR arrays at the Newell County carbon storage facility: four years and continuing

Kevin D. Hutchenson¹, Jonathon Yelton¹, Derek Quigley¹, Elige “Buck” Grant¹,
Paul A. Nyffenegger¹, Mike Dahl², and Brett Frederiksen²

¹ Geospace Technologies, Inc., ² Geospace Technologies Canada, Inc.

Summary

Traditional methods for seismic MMV of the area of review identified for GCS sites use networks of surface sensors and downhole sensor strings (Eaton, 2018; Maxwell, 2014). These passive monitoring approaches are in wide use in a variety of production and disposal facilities. Our approach is to use a sparse network of volumetric phased arrays, designed for the area in question, as an alternative.

These SADAR arrays have been shown to be robust and reliable over a nearly four-year recording period.

Introduction

Traditional methods for seismic MMV of the area of review identified for GCS sites use networks of surface sensors and downhole sensor strings (Eaton, 2018; Maxwell, 2014). These passive monitoring approaches are in wide use in a variety of production and disposal facilities. Surface sensors have issues with signal-to-noise (SNR) and wells for downhole sensor strings can be sparse in many areas, insufficient for effective monitoring.

Downhole borehole strings on wirelines may be the most common (Maxwell, 2014, 2010), although cemented arrays in boreholes is also common (Maxwell, 2014; Smith, 2010). The advantage is placement near sources for VSP or crossline. Fields of shallow sensors installed in gridlines or radial lines away from treatment wellheads are also common (Maxwell, 2014). Each of these have advantages (near source) and disadvantages (boreholes are few and expensive; near surface has increased noise).

Sparse networks of permanently emplaced SADAR phased arrays represent a fundamentally different approach for reservoir surveillance. SADAR systems provide superior data and information compared to surface networks and downhole strings, providing true phase velocities and accurate azimuths and dips for the arriving wavefront not provided by traditional planar systems. The SADAR arrays are deployed in shallow boreholes below the weathering layer taking advantage of this layer for damping the industrial noise fields. With burial effectively increasing the signal-to-noise ratio (SNR) compared to surface sensors, and the gains provided by coherent processing (beamforming), the result is lower magnitude microseismic detection thresholds over larger geologic volumes with more certain locations while occupying a smaller footprint.

The SADAR technology can be utilized in many applications where microseismic monitoring is needed. SADAR array field components and system design provide redundancy protection against sensor attrition without a loss of key capabilities for monitoring. A record from 47 months of passive microseismic monitoring are presented in this study.

Method

In November 2021, Quantum Technology Sciences installed a sparse network of four dual-use permanent SADAR arrays at Carbon Management Canada's Field Research Station (FRS) proving ground (Macquet *et al.*, 2022; Lawton *et al.*, 2019) to demonstrate compact volumetric phased arrays for seismic MMV at an active GCS facility (Nyffenegger *et al.*, 2025a,b; Hutchenson *et al.*, 2025a,b; Nyffenegger *et al.*, 2023; Zhang *et al.*, 2023; Nyffenegger *et al.*, 2022). The elements of the uniform cylindrical array variants are comprised of vertical 10 Hz geophones installed in shallow boreholes between 9m-19m depth and grouted in place; the vertical extent of the arrays is contained within the Pleistocene-Holocene sediment and glacial till layer below the weathering zone just above the competent strata. SADAR array field components and system design provide redundancy protection against sensor attrition without a loss of key capabilities for either passive or active-source monitoring (Hutchenson *et al.*, 2025b; Quigley *et al.*, 2025).

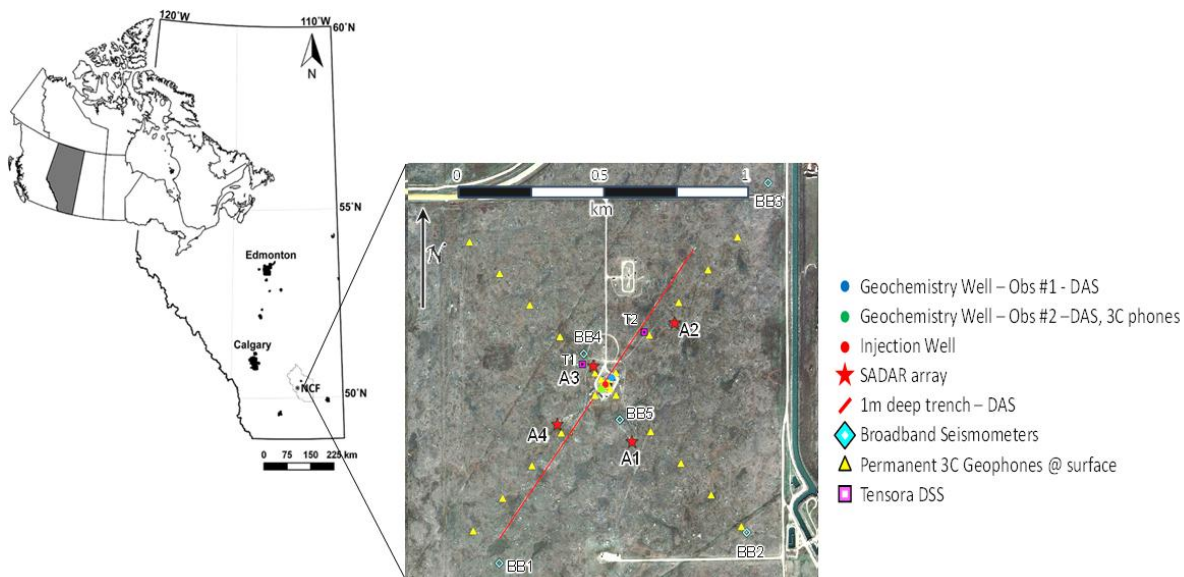


Figure 1. Location of the CMC FRS in Alberta. The four SADAR arrays (red stars) are shown dispersed around the injection well (red circle), labeled as A1 to A4.

Installation of the four arrays took about a week to obtain operational status. For the 47-month recording period, the system has been operating at or above 99% with no downtime for maintenance. All sensors are wired to a central recording facility with a backup recording disk, and GPS timing.

One of the key features of the SADAR arrays is their burial, between 9 m and 19 m, beneath the weathering layer. This depth avoids much of the noise typically observed in sensors near the surface. The depth placement reduces much of the surface noise.

The recording architecture is ideal for incorporating a processing pipeline, with signal conditioning, detectors for phase picks with associated pick uncertainty, location, and magnitude calculations. The system hardware at the site is currently unable to run a pipeline process; the pipeline is run on the data at another site, but it has been tested and demonstrated at the site.

During one period, a planar 3C array was placed on the surface above one of the arrays. The planar array consisted of GS-ONE 10 Hz 3C geophones (GCL) while the SADAR arrays consist of only vertical GS-ONE 10 Hz geophones.

Results

Results from monitoring are shown in Figure 2. The figure shows 741 events recorded by all four SADAR arrays during the 47-month period. Events shallower than 15 m are NOT shown; many of these represent surface clutter. There is no clear way to separate known surface clutter from shallower events. Note many of the events cluster near the injection well.

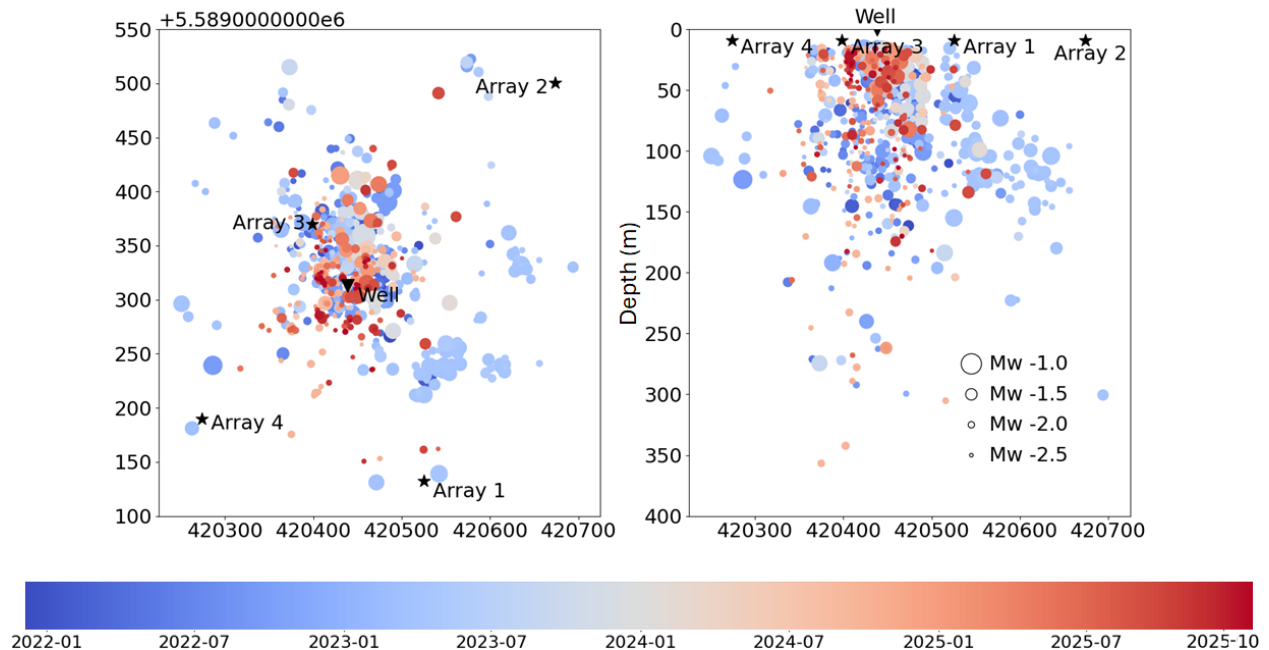


Figure 2. Spatial distribution of events recorded by the sparse SADAR network (left) and with depth (right). There are 741 events located using the four SADAR array events whose depths are deeper than 15 km.

The moment magnitude (Mw) distribution for this same period (Figure 3, left). The magnitudes are calculated following the Brune method (1970, 1971). In addition, the signal power vs. the source-receiver for the 741 events are color coded by Mw for the same time period for events with $z > 15$ m (Figure 3, right). The solid lines represent signal levels adjusted for propagation loss; dashed lines represent noise thresholds.

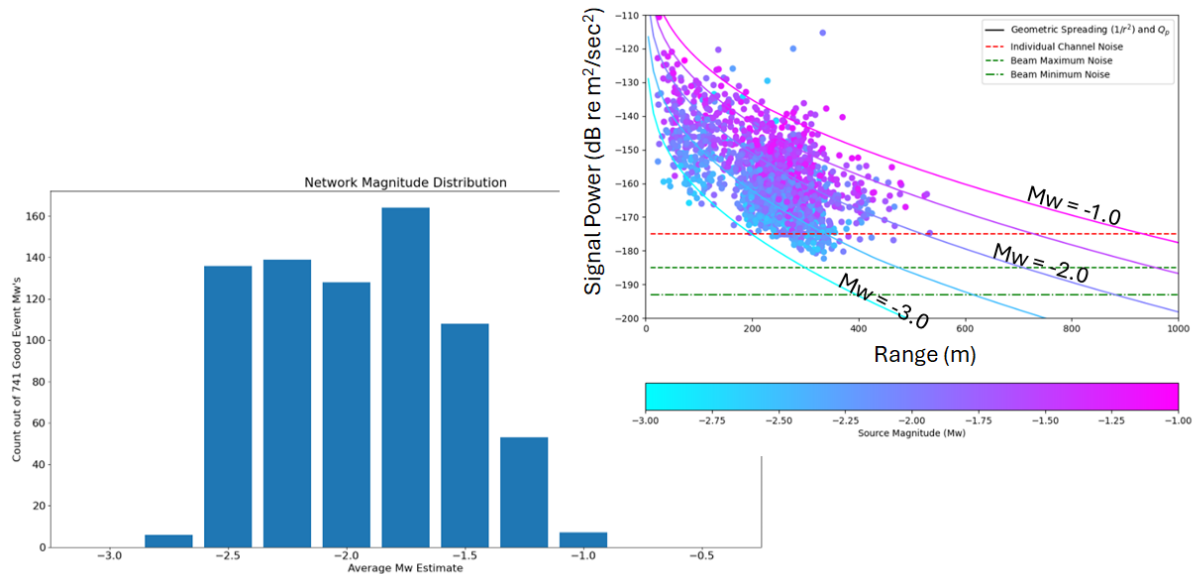


Figure 3. Spatial distribution of event magnitude (M_w) recorded by the sparse SADAR network (left). M_w is calculated following the Brune (1970, 1971) method for the 741 events. On the right, signal power vs. source-receiver. Solid lines are adjusted for propagation loss; dashed lines represent noise thresholds.

During this deployment, an opportunity existed to compare the noise difference between a surface sensor array and the buried SADAR sensors. A surface array was installed over the buried SADAR array with nearly identical sensors (Figure 4), GS-ONE 10 Hz 3C geophones (GCL) while the SADAR arrays consist of only vertical GS-ONE 10 Hz geophones. Two time periods were tested, including local midnight and local noon (Figure 4).

As expected, the surface sensors have greater noise levels at more frequency bands compared to the SADAR array individual sensors (Hutchenson *et al.*, 2025). This is the local noon time range; theoretically the most noisy part of the day. The use of the beam to reduce the noise, increase the signal-to-noise ratio, is significant. Combining the surface sensors is not as dramatic.

Note the strong spikes on the SADAR data. These are associated with electrical line noise. Spikes on the surface sensors are not; these sensors are battery powered. These spikes are associated with machinery running on the compound. Array 3 is 70 m from the injection well.

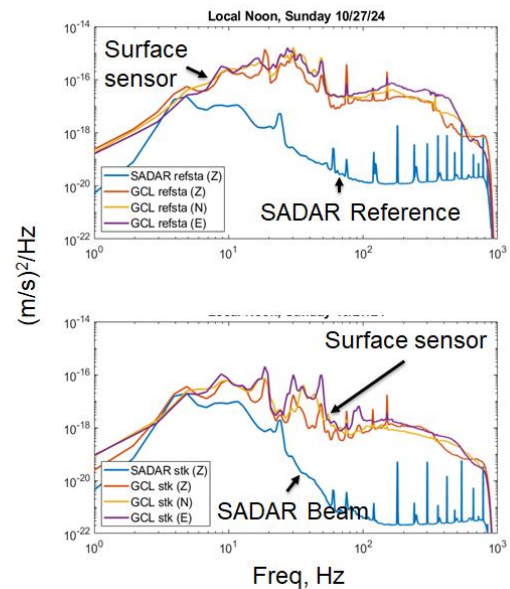


Figure 4. (left) Spatial view of the Array 3. The SADAR borehole sensors are located at the positions of the triangles (green), buried at depths of 9, 11, and 13 m. The surface patch array are shown at the positions of the squares (white). (right) Spectra calculated for the surface sensors and buried SADAR sensors. The top shows individual sensor; the bottom shows the results of the beam.

To address the reliability of the SADAR systems, experimental sensor loss trial results for robustness were undertaken for the phased array. The results show the measured attributes are not greatly degraded through loss of 15 sensors (27% of total). Azimuth and dip measurement deviations average $\sim 5^\circ$ and measured phase velocity deviations average ~ 50 to 75 m/s. Degradation of array gain against random noise is estimated within ~ 1.5 dB difference (not shown). Larger deviations become apparent only after losses of 20 or more sensors (Hutchenson *et al.*, 2025b).

Conclusions

The sparse SADAR network is demonstrated as a very effective system for microseismic monitoring, delivering consistent event bulletin with locations, uncertainties, and attributes continuously since its installation. The network provides a persistent coverage of $\sim 156,000$ m² surface area using a small footprint of only ~ 150 m².

The reduced footprint means less area will need to be available for installation. Even so, the sparse network of SADAR arrays monitors much larger areas, scalable upwards with additional arrays to monitor an expanding area of review as need expands.

Robustness and reliability of the SADAR has been demonstrated by deployed time in the field and experimental results using actual data from the arrays. The SADAR system reduces operational and financial risks for GCS monitoring with robust system components and array design and provides the ability to operate continuously under industrial noise conditions.

Although not shown during this presentation, a dual use capability exists. The arrays are capable to imaging the area resulting from active vibroseis lines. The dual-use capability of the arrays is reported in Hutchenson *et al.*, 2025 and Quigley *et al.*, 2025.

Acknowledgements

Geospace Technologies thanks to Carbon Management Canada for access to the Newell County Field Research Station, operational data, and support for SADAR system installation. The facility is funded by the Joint Industry Project.

References

- Brune, J., 1971, Correction: *Journal of Geophysical Research*, **76**, 5002.
- Brune, J., 1970, Tectonic stress and the spectra of seismic shear waves from earthquakes: *Journal of Geophysical Research*, **75**, 4997-5009.
- Eaton, D., 2018, *Passive Seismic Monitoring of Induced Seismicity*: Cambridge University Press, New York.
- Hutchenson, K.D., D. Quigley, J. Yelton, E.B. Grant, and P.A. Nyffenegger, 2025a, Capabilities of microseismic monitoring using robust permanent SADAR arrays: presented at IMAGE 2026, Houston, TX.
- Hutchenson, K.D., J. Jennings, E.B. Grant, D. Quigley, J. Yelton, and P.A. Nyffenegger, 2025b, Persistent microseismic monitoring using robust permanent SADAR arrays: presented at CCUS 2025, Houston, TX.
- Hutchenson, K.D., D. Quigley, J. Longbow, E.B. Grant, P.A. Nyffenegger, J. Jennings, M.A. Tinker, M. Dahl, D. Grindell, M. Macquet, and D.C. Lawton, 2023, Microseismic monitoring using SADAR arrays at the Newell County carbon storage facility: what have we learned in a year?: Presented at GeoConvention, 2023, Calgary.
- Lawton, D.C., J. Dongas, K. Osadetz, A. Saeedfar, and M. Macquet, 2019, Chapter 16: Development and analysis of a geostatic model for shallow CO₂ injection at the Field Research Station, Southern Alberta, Canada: *in* T. Davis, M. Landro, and M. Wilson, eds., *Geophysics and Geosequestration*: Cambridge University Press, 280-296. DOI 10.1017/9781316480724.017.
- Macquet, M., D. Lawton, K. Osadetz, G. Maidment, M. Bertram, K. Hall, B. Kolkman-Quinn, J. Monsegny Parra, F. Race, G. Savard, and Y. Wang, 2022, Overview of Carbon Management Canada's pilot-scale CO₂ injection site for developing and testing monitoring technologies for carbon capture and storage, and methane detection: *CSEG Recorder*, **47**, No. 01.
- Maxwell, S., 2014, Microseismic imaging of hydraulic fracturing: Improved engineering of unconventional shale reservoirs: Distinguished instructor series, No. 17, SEG.197 pp.
- Maxwell, S.C., 2010, Microseismic: Growth born from success: *The Leading Edge*, **29**, 338-343.
- Nyffenegger, P.A., K.D. Hutchenson, Derek Quigley, Jon Yelton, Mike Dahl, 2025a, Integrated Passive and Active Source Sparse Seismic Monitoring for Geologic Carbon Storage Projects: presented at IMAGE 2026, Houston, TX.
- Nyffenegger, P.A., D.C. Lawton, M. Macquet, D. Quigley, B. Kolkman-Quinn, and K.D. Hutchenson, 2025b, Advances in coupled passive and active seismic monitoring for large-scale geologic carbon storage projects: *in* Wilson, M., T. Davis, and M. Landro, eds., *Geophysics and the Energy Transition*: Elsevier Press, 333-354.
- Nyffenegger, P.A., J. Zhang, E.B. Grant, D. Quigley, K.D. Hutchenson, M.A. Tinker, D.C. Lawton, and M. Macquet, 2023a, Performance and outlook for the SADAR array network at the Newell County Facility: *First Break*, **41**, 56-62.
- Nyffenegger, P.A., M.A. Tinker, J. Zhang, E.B. Grant, K.D. Hutchenson, and D.C. Lawton, 2022, Compact phased arrays for microseismic monitoring: *First Break*, **40**, 69-74.
- Quigley, D., P. A. Nyffenegger, K. D. Hutchenson, J. Yelton, 2025, Active source sparse imaging using permanent SADAR arrays: presented at CCUS 2025, Houston, TX.
- Smith, R.J., 2010, 15 years of passive seismic monitoring at Cold Lake, Alberta: *CSEG Recorder*, 35.
- Zhang, J., K.D. Hutchenson, P.A. Nyffenegger, E.B. Grant, J. Jennings, M.A. Tinker, M. Macquet, and D.C. Lawton, 2023, Performance comparison of compact phased arrays and traditional seismic networks for microseismic monitoring at a CO₂ sequestration test site: *The Leading Edge*, **42**(5), 332-342.